Genomic rearrangements rewire chromatin contacts and drive adaptive gene expression divergence in mammals

Jui Bhattacharya, Mohan Lal, Kuljeet Singh Sandhu*

Department of Biological Sciences
Indian Institute of Science Education and Research (IISER)- Mohali
Knowledge City, Sector 81, SAS Nagar 140306, Punjab, India.

*sandhuks@iisermohali.ac.in

Keywords: Genomic rearrangements, mammalian evolution, clade-specific traits

Running title: Adaptive genome rewiring in mammals

Abstract
Genomic rearrangements (GRs) are pervasive in mammalian evolution, yet their contribution to adaptive trait divergence remains poorly defined. By examining 71 mammalian genomes across eight major clades, we uncovered 206 clade-specific disruptions of ancestral synteny. These rearrangements consistently localize near genes underpinning clade-specific physiological, metabolic and behavioural traits and coincided with the accelerated expression rates in the affected lineage. The disruption of otherwise syntenic chromatin contacts and the fusion of domains with contrasting epigenetic states underlie the expression divergence. These observations imply that the clade-specific genomic rearrangements repeatedly reconfigured the mammalian regulatory landscape and likely served as an evolutionary substrate for lineage-specific adaptation.

Introduction

Genomes have gone through several rounds of structural rearrangements during the course of evolution. These rearrangements reshape the genome order and, therefore, may change the regulatory context of the genes. Such alterations may lead to expression divergence, of genes popularly known as chromosomal position effect(Elgin and Reuter 2013; Wallrath and Elgin 1995). Ectopic position effects can lead to diseases in human and mice(Kleinjan and Van Heyningen 1998; Milot et al. 1996). For example, translocation breakpoint between PAX6 and its downstream regulatory elements associates with Aniridia in human(Fantes et al. 1995). A genomic rearrangement at 100kb upstream to Steel(Sl) locus downregulates Mgf gene and causes sterility in female mice(Bedell et al. 1995) . Similarly breakpoints near SOX9, TWIST, and RIEG genes have association with campomelic dysplasia, Saethre-Chotzen, and Rieger syndromes respectively in human(Wirth et al. 1996; Krebs 1997; Flomen et al. 1998). Yet the evolutionary implications of chromosomal position effects remain largely under appreciated. De et al had shown that expression divergence associated with the position effects may contribute to phenotypic differences between human and chimpanzee(De et al. 2009). Bagadia et al showed that the genomic rearrangements may explain the evolutionary divergence of some brain related traits in rodents(Bagadia et al. 2019). Recently, Real et al(Real et al. 2020) identified genomic rearrangements that altered the regulatory context of gonadal gene expression governing intersexuality in moles. These studies were limited by the number of species analysed and by the context of genomic rearrangements. With the availability of large number of mammalian genomes, it is now possible to examine the phenotypic associations of genomic rearrangements in mammals. Through analysis of 71 mammalian genomes representing 8 clades, we identified 206 clade-specific long-range genomic rearrangements marking evolutionary loss of synteny. We found that the clade-specific breakpoints flanked by the genes associated with specific phenotypes of respective clades. The clade-specific breakpoints frequently disrupted the conserved enhancer-promoter communications, which coincided with the diverged expression rates of the flanking genes. Our observations implied the wide-spread adaptive significance of genomic rearrangements in mammals.

Results

By applying the strategy outlined in the Methods section, we identified 206 clade-specific instances of long range (>10 Mb and *trans*) genomic disruptions of synteny across 71 mammals(Figure 1a-c). More than 90% of gene-pairs flanking clade-specific breakpoints were syntenic in the eutherian ancestor(Kim et al. 2017), validating our inference of ancestrally syntenic configuration of the identified cases (Figure S1). Artiodactyls and rodents presented the greatest number of clade-specific loss-of-synteny (cs-LoS) events (38 and 94 respectively), which was consistent with the earlier reports(Kim et al. 2017; Luo et al. 2012).

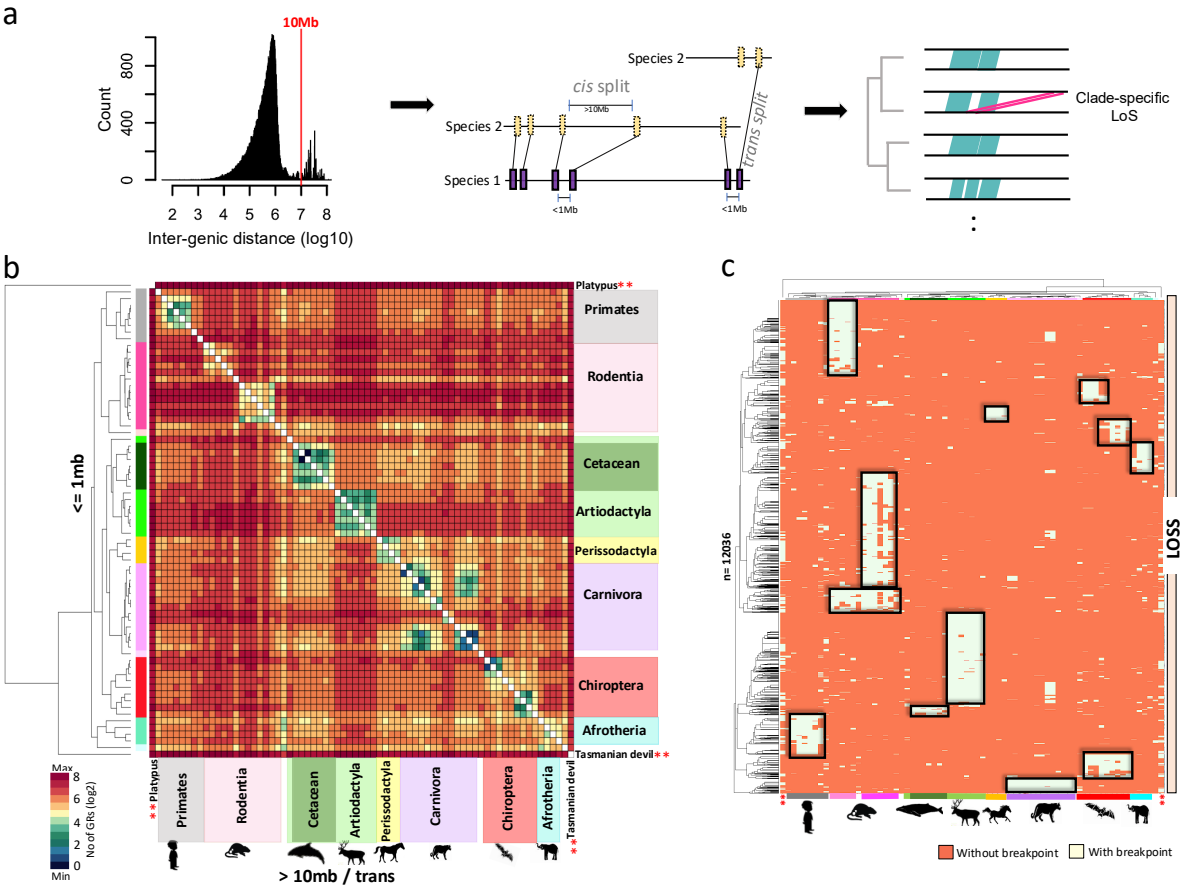

Figure 1. Inference of clade-specific loss of synteny events across mammalian lineages. (a) Schematic representation of the strategy to define the clade-specific loss of synteny events. The distribution plot of genomic distance between adjacent genes in a species, which were <1 Mb apart in another species. Vertical line demarcates the separation of gene-pairs by >10mb in a species. **(b)** Heatmap representation of number of genomic rearrangements between lineages **(c)** Inferred clade-specific loss of synteny (LoS) events. Highlighted in rectangles are the clade-specific LoS events.

To assess if the cs-LoS EBRs position preferably near certain functional loci, we obtained the genes within and the flanking 10 genes on the either sides of cs-LoS EBRs. Gene ontology analysis yielded enrichment of clade-specific functional terms. Primates exhibited enrichment of glucocorticoid secretion (CRHR1, TAC1, CRY1 etc.), lipid transport, synaptic transmission and behaviour related terms (SHANK2, RELN, FOXP1, GIT1, KLHL1, NRG1, MAPT etc.) (Figure 2). These functions have associations with primate-specific trait divergence(Dunn-Fletcher et al. 2018; Bozek et al. 2015; Spanaki et al. 2024; Muntané et al. 2015). The genes flanking artiodactyl-specific LoS break-points were enriched with flavonoid and lipid metabolism related terms, including genes like UDP-glucuronosyltransferase 1A (UGT1A) and Fatty Acid Binding Protein 4 (FABP4) (Figure 2). These terms associate with vegetarian diet and musculoskeletal health respectively, which coincide with herbivory and relatively large body mass of artiodactyls(Jiang et al. 2014; Kawai et al. 2021). Carnivore-specific LoS exhibited enrichment of extra-cellular matrix proteins, particularly matrix metalloproteases (MMPs) (Figure 2). It is established that carnivores, unlike other mammals, have endotheliochorial placenta(Wooding and Burton 2008). Differential expression of MMPs is the hallmark

of invasive placentation in carnivores(Diessler et al. 2017). We further hypothesize that enrichment and expression divergence of MMPs in carnivores may also relate to effective wound healing in carnivores being susceptible to frequent wounds due to predation and the territory defence. Rodents exhibited enrichment of renal filtration related terms, aligning to their higher glomerular filtration rate, which is an adaptation to physiological requirements in diverse habitats and dietary habits of rodents(Benjamin et al. 2015; Dickinson et al. 2007; Bittner et al. 2021). The term includes the genes Anillin, Glucocorticoid Induced 1 (GLCCI1), Thrombospondin

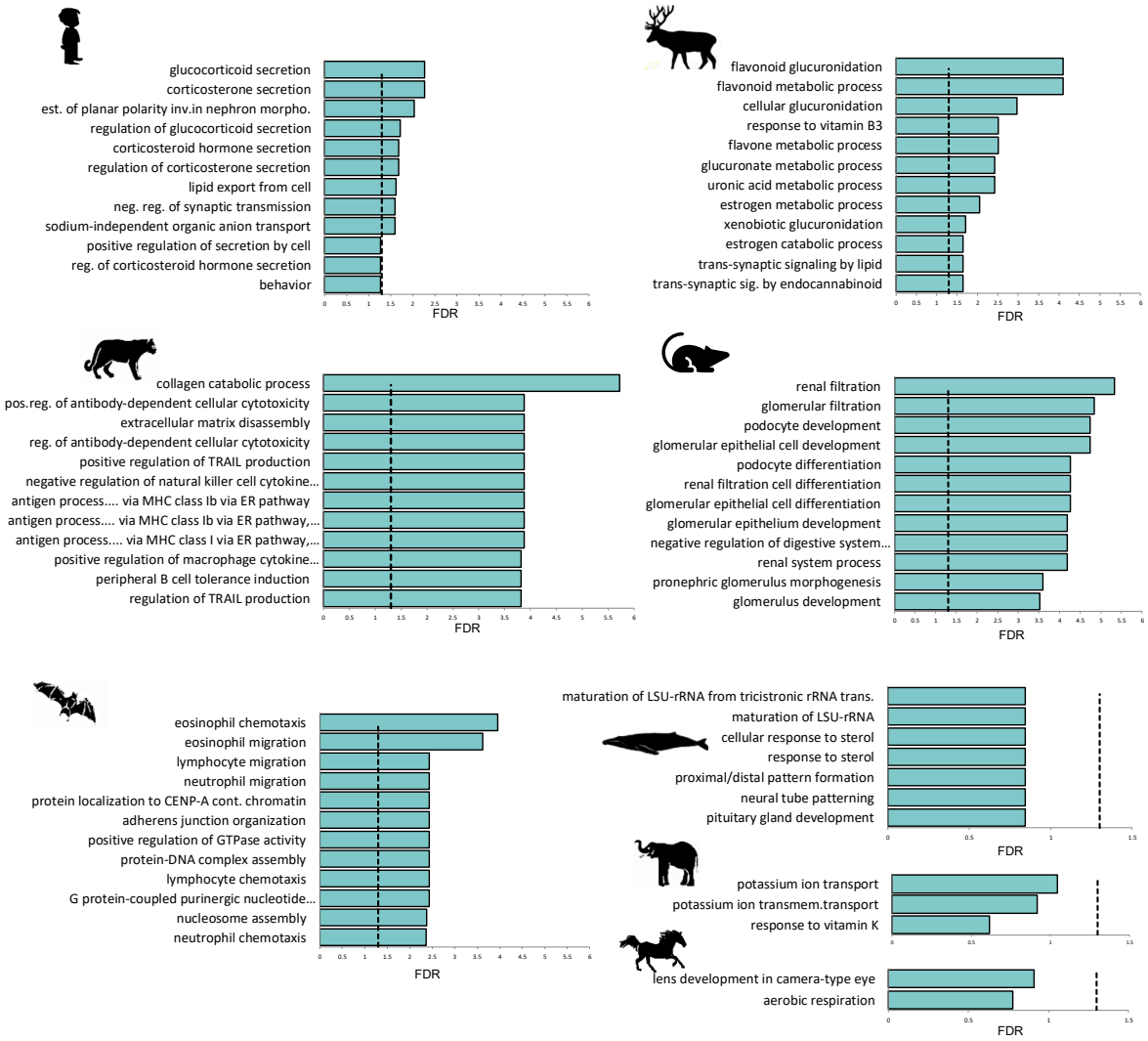

Figure 2. Functional associations of synteny disruptions. Enrichment of GO Biological Process terms among genes flanking the clade-specific EBRs. We implemented Benjamini-Hochberg correction of multiple testing. FDRs on the x-axis are converted to -log10 scale. The vertical lines mark the FDRs of 0.05.

type-1 domain-containing 7A (THSD7A), Apolipoprotein L1 (APOL1) etc., which have strong associations with renal filtration and implicate in kidney diseases(Gbadegesin et al. 2014; Nishibori et al. 2011; Tomas et al. 2014; Pays 2021). Top enriched

genes in Chiroptera-specific LoS break-points exhibited immunity related functions, adhering to pronounced immune tolerance in bats(Jebb et al. 2020; Sulak et al. 2016). Among others, we also observed genes like CEBPA and TNFRSF1A that are associated with echolocation in bats(Hudson et al. 2014; Wang et al. 2019). The cetacean break-points show weak enrichment of r-RNA processing and sterol related functions, aligning to longevity, body mass and diverged metabolism of cetaceans(Doherty and de Magalhães 2016; Derous et al. 2021) Afrotheria-specific LoS showed moderate enrichment of potassium ion channels, vitamin-K metabolism, and the blood coagulation (Figure 2). Ion transporters are linked to the cell proliferation, cell size and cancer, the traits significantly diverged in afrotheria clade(Savage et al. 2007). Vitamin-K is linked to the osteoblast differentiation, likely associated with the larger body mass of afrotherians like elephant, manatee etc. Blood coagulates faster in elephants(Lewis 1974) and the presence of blood coagulation factors in our set might mark an adaptation against an ancient fatal haemorrhagic disease caused by elephant endotheliotropic herpesvirus(Guntawang et al. 2021). Similarly, perissodactyl-specific breakpoints showed moderate enrichment of eye development and aerobic respiration, which lines up with the large size, 350° visual field and unique motion sensitivity of horse eye(Roth and McGreevy 2025), and remarkably high aerobic respiration capacity of equine lungs(Poole and Erickson 2011) (Figure 2).

In most clades, genes proximal to the cs-LoS breakpoints exhibited the expression divergence from that of the phylogenetically proximal clade controlled through an outgroup, implying the adaptive significance of genomic rearrangements (Figure 3a). The chromosomal position-effect may explain the observed expression divergence. To test this, we first analysed the chromosomal coordinates of enhancer-promoter pairs that exhibited evolutionarily conserved synteny. We observed non-random accumulation of clade-specific breakpoints within enhancer-promoter spans, which were syntenic in other clades, suggesting that the expression divergence of genes might have been driven by the loss of proximity to their cognate enhancers (Figure 3b-c). secondly, we assessed the position effect through analysis of chromatin compartments. We observed that the chromatin compartments with contrasting states (A and B) in a species tended to fuse together and subsequently exhibited a coherent state (A or B) in the species exhibiting cs-LoS event (Figure 3d-e). This is marked by a decrease in Kronecker's delta (Methods) of consecutive genomic bins around breakpoints (Figure 3d). This may signify an alteration in gene expression through the mixing of contrasting epigenetic states *via* gained proximity. We illustrated this through an example of primate-specific genomic rearrangement near Neurokinin-1 (TAC1), a glucocorticoid secretion and behaviour related gene. The gene locates in the B-compartment in mouse, which gains proximity to an A-compartment, and subsequently switches from B-to-A compartment in neuronal cells (Figure 3e). Overall the split of enhancer-promoter synteny and gain of proximity between A and B chromatin compartments highlight the mechanistic basis of expression divergence of genes located near cs-LoS breakpoints.

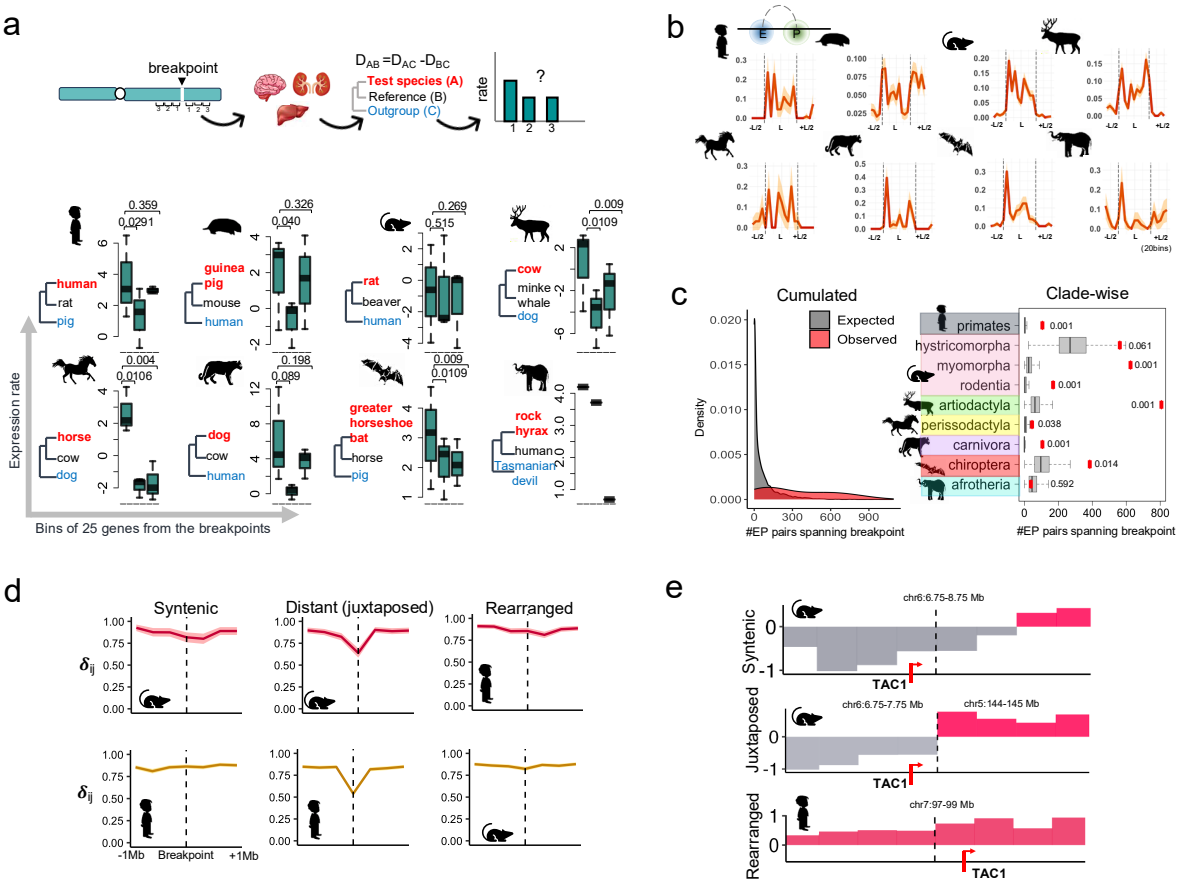

Figure 3. Chromosomal position effect associated with the clade-specific loss of synteny. (a) Lineage-specific expression divergence of the genes as a function of distance from the clade-specific evolutionary break-points, calculated assuming Ornstein-Uhlenbeck model of transcriptome evolution. Each box represents the distribution of expression divergence values of 25 genes incrementally distant from the breakpoint. A species from the nearest order or sub-order was taken as reference species, while a species hierarchically outside the clade of test and the reference species was taken as outgroup species. (b) Enrichment of clade-specific breakpoints within and around enhancer-promoter loops in the species having syntenic configuration. Loop coordinates were extended either side by half of the loop length-L (b) The number of conserved enhancer-promoter contacts that had lost proximity through GR in a clade-specific manner, superimposed onto the random null distribution obtained from controlled randomized of breakpoints. P-values are calculated using bootstrap method. Shown are the plots for the cumulated set and the clade-specific sets. (d) Kronecker's δ_{ij}, signifying change in A and B compartment states of neighbouring domains, as a function of distance from the break-points in primates and rodents. Drop in Kronecker's delta signifies the switch in states (A-to-B or B-to-A). The three plots correspond to syntenic configuration in mouse (left), distal regions (syntenic in human) when juxtaposed in mouse (middle), rearranged syntenic regions in human (right) respectively in case of primate-specific LoS. Similarly, for rodent-specific LoS, syntenic configuration in human (left), distal juxtaposed regions in human (middle) and rearranged syntenic regions in mouse (right) are plotted. Chromatin compartment states (leading Eigen vector of Hi-C contact matrix) for regions around TAC1 locus, which exhibited primate-specific LoS nearby, in mouse and human neuronal cells. A and B compartments are coloured as red and grey colours respectively.

We further exemplified a primate-specific LoS event near Corticotropin Releasing Hormone Receptor 1 (CRHR1) gene that coordinates the autonomic, endocrine and behavioural response to stress and depression through Hypothalamus-Pituitary-

Adrenal (HPA) axis(Jezova et al. 1999) and may also regulate the timing of birth(Smith and Nicholson 2007). Interestingly, CRHR1 shows primate-specific conservation of 29 amino acids of exon-6, and insertions of retroviral LINE elements at the upstream region (Figure S2). The gene also exhibits loss of chromatin contacts and expression divergence in primates (Figure 4). We propose that the sequence and the expression divergence of this locus may link to primates' adaptation to stress from complex social structures(Pusey et al. 1997; Sapolsky 2021). Similarly, artiodactyl-specific LoS near UGT1A genes, which metabolizes flavonoids commonly present in vegetarian diet, exhibited disruption of chromatin contacts and expression divergence in artiodactyls (Figure 2f-g). UGT1A genes have expanded copy numbers in herbivores(Kawai et al. 2021), implying convergence of distinct molecular mechanisms underlying expression evolution of UGT1A genes in artiodactyls.

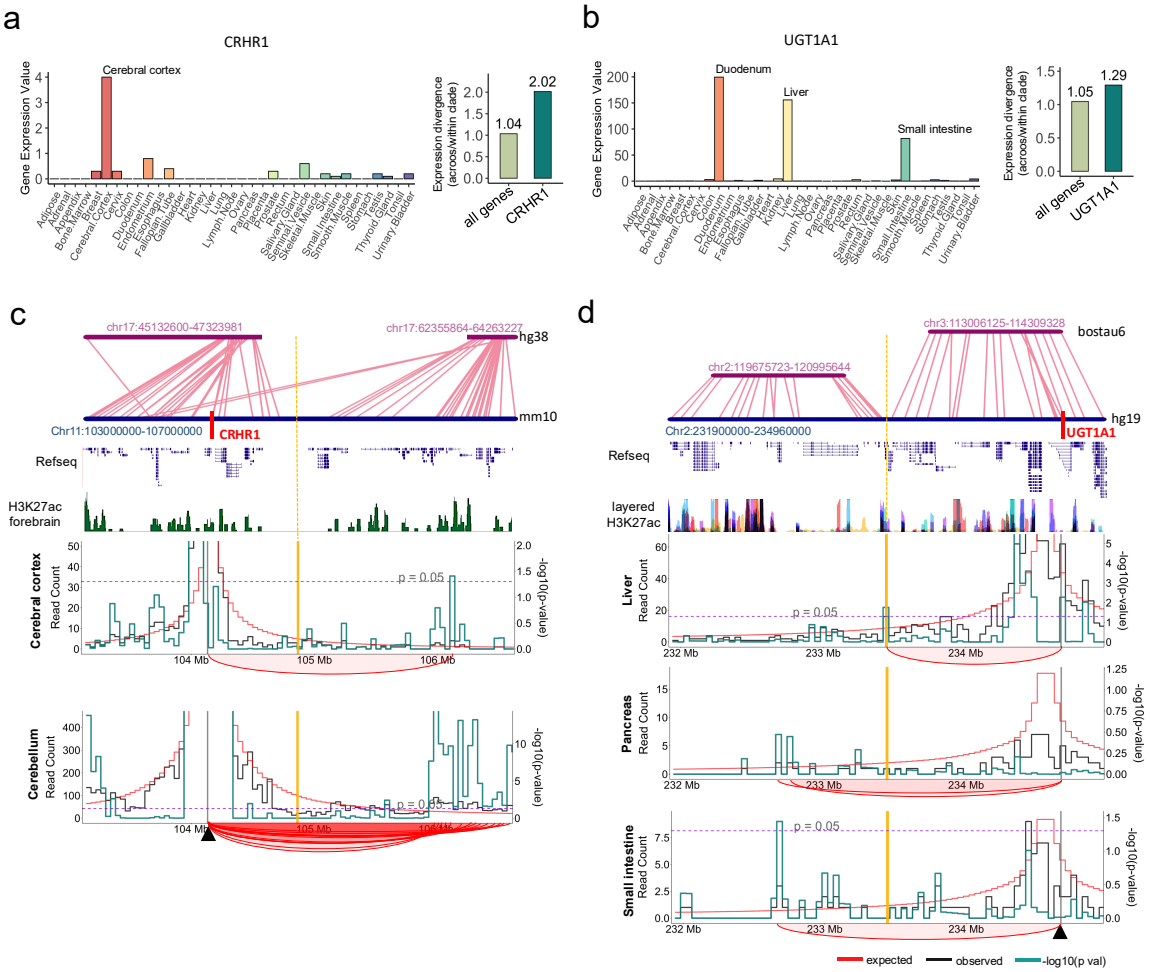

Figure 4. Illustrative examples of clade-specific breakpoints.(a-b) Left-panels: CRHR1 and UGT1A expression values in 35 human tissues respectively. Right-panels: expression divergence calculated as the Euclidean distance across tissues and summarized as ratio of across-clade to within-clade distances.(b-c) Mouse-to-human and human-to-cow synteny plots around (b) CRHR1, and (c) UGT1A gene respectively. Shown below are the tracks of RefSeq non-redundant genes, H3K27ac modification, and virtual 4C in relevant tissues. The clade-specific break-point regions are highlighted by vertical bars. 4C reference loci are highlighted using arrow-heads. Black and red curves represent observed and expected 4C signals respectively. Green curve represents -log10 of p-values. Blue dashed line represents the p-value cut-off of 0.05. Red arcs mark the significantly frequent chromatin contacts.

Discussion

Genes are not autonomous transcriptional units within the genomic landscape but rather operate in a highly context-dependent manner influenced by their local and global chromatin environment. Reporter integration in proximity to enhancer strengthens the expression, while that within lamina-associated domains attenuates the transcriptional activity(Akhtar et al. 2013). Distinct linear and spatial positions of a gene also confer variation to its expression noise(Chen and Zhang 2016; Singh et al. 2016). The alterations in genomic context through chromosomal rearrangements can, therefore, influence the epigenetic and transcriptional states of the genes. Although studied in somatic human cells and cancer tissues(Chiang et al. 2017; Xu et al. 2022), the evolutionary dynamics of such position effects remains poorly understood. Our observations through this study highlight that the clade-specific long-range genomic rearrangements associate with the enrichment and expression-divergence of genes with clade-defining traits. Interestingly, these genes have also lost the proximity to their cognate enhancers as reflected from the splitting of enhancer-promoter pairs, likely representing one of the possible causes of the observed divergence of gene expression in the respective clades. The gained proximity of chromatin domains with opposing epigenetic states further strengthens the notion of chromosomal position effect in evolutionary context. We propose that the alteration in regulatory context may have contributed to the expression evolution of genes proximal to clade-specific EBRs. From our observations, it follows that clade-specific GRs may have guided the evolution of clade-specific mammalian phenotypes through gene expression evolution. While largely correlative in nature, our observation may guide future experiments and help designing genetic manipulations in closely related species to test the causal associations.

The reported genomic rearrangements and the engaged loci also offer a valuable resource to prioritize biomedical research. Many of the reported loci also implicate in human diseases and understanding the rewiring of their regulatory contexts could help in genetic prioritization and devising medical strategies to intervene the mis-regulation. Certain mammals are resistant to certain diseases, like elephant is resistant to cancer and bats are immune tolerant to viruses. Our observations may also help studying the regulatory contexts which are instrumental in disease resistance and exploit that knowledge to understand disease susceptibilities in humans.

Conclusion

Altogether, our observations suggest that clade-specific genomic rearrangements are not merely the passive signatures of evolutionary history and speciation but are active agents reshaping mammalian regulatory landscapes. By rewiring enhancer-promoter contacts and shuffling chromatin compartments, these rearrangements generate lineage-specific expression programs that coincide with the emergence of clade-defining phenotypes. The recurrence of such events across distant mammalian clades highlights genome topology as a pervasive, yet underappreciated, substrate of adaptive evolution. Together, our results establish long-range genomic rearrangements as an important evolutionary force that has repeatedly sculpted mammalian diversity.

Methods

Genome data

We obtained the chromosomal coordinates of human orthologous genes for 18 mammalian species from Ensembl (http://www.ensembl.org). Fifty three genomes not represented in Ensemble were obtained from DNA Zoo (https://www.dnazoo.org/assemblies) and Bat1K Project (https://bat1k.com/). We aligned the genome FASTA files to the human genome using LASTAL(https://github.com/lpryszcz/last). Resulting maf files were processed with *'last-split'* and converted to chain files using *'maf-convert'* utility (https://github.com/lpryszcz/last). To obtain orthologous genomic coordinates, we used the UCSC LiftOver tool (https://genome.ucsc.edu/cgi-bin/hgLiftOver). The phylogenetic tree of the species is given in the Figure S3. The genome assembly information is provided in Dataset S1.

Identification of clade-specific loss-of-synteny (LoS) events

To define evolutionary breakpoints of long-range genomic rearrangements, we used a distance-based approach. For each species, we first calculated linear distances between non-redundant all possible *cis* gene pairs. Gene pairs separated by ≤1 Mb were considered syntenic in a given species. The corresponding intergenic distances between orthologues of these syntenic pairs were then obtained for all other species and their distribution was visualized as histograms using the 'hist', function in R. The analysis revealed a bimodal distribution with two modes separated at around 10 Mb distance. This 10 Mb threshold was, therefore, used as a threshold to define loss of synteny events. Gene pairs that were within 1 mb distance in one species but exceeded 10Mb in other species were categorized as *cis*-rearrangement. If the orthologues of syntenic pairs were located on different chromosomes in another species, they were classified as *trans*-rearrangements. To minimize noise that might result from retro-transposition or assembly errors, we further obtained the set where the orthologous disruption occurred with at least 3 genes on either side of the break-point. We further calculated the inter-breakpoint distances defined as the linear distances between gene pairs forming breakpoints across all species. The distribution of distances suggested a distinct natural cut-off of 1.4 Mb (Figure S4), below which the breakpoints can be considered as clustered into evolutionary break-point region (EBRs). An EBR was identified as a clade-specific loss-of-synteny (LoS) event if it engages in LoS events in at least 50% of the species within a given mammalian clade, while being syntenic in most other clades (split in not more than two species).

Gene Ontology analysis

For each evolutionary breakpoint region (EBR), we extracted all genes within EBR and 10 genes upstream and downstream of both ends. These unique gene sets were compiled for each clade. Gene ontology (GO) enrichment analysis was performed using the ToppFun function from the ToppGene Suite (https://toppgene.cchmc.org/) to fetch the GO Biological Process categories. P-values were corrected using Benjamini-Hoschberg method.

Gene expression analysis

We retrieved the expression data of CRHR1 and UGT1A1 of 35 human tissues from the TissueEnrich database(https://tissueenrich.gdcb.iastate.edu/) for tissue specific

gene enrichment analysis. To calculate expression divergence, we used tissue-wide expression data from the Bgee database(https://www.bgee.org/). For each gene (CRHR1 and UGT1A1), a divergence ratio was calculated as the median of across-clade versus within-clade distances. These gene-specific ratios were compared to the genome-wide median divergence ratios calculated across all genes.

Expression rate analysis

We used 'TreeExp' R-package(https://github.com/hr1912/TreeExp) to evaluate the evolutionary rates of expression divergence assuming Ornstein-Uhlenbeck model of gene expression evolution. For each clade, we assigned a test species, a reference species and an out-group species from phylogenetically adjacent clade. We made three distance-based bins, each comprised of 25 genes, on either side of the break-point. Gene expression data were obtained from Liu et al(Liu et al. 2023), which provides expression profiles for three tissues: brain, kidney, and liver for multiple species.

Enhancer-promoter contact analysis

All human enhancer-promoter (EP) pairs and their orthologues in other species, were obtained from the dataset provided by Laverré et al(Laverré et al. 2022). The evolutionarily conserved EP pairs were then used to analyze disruption by clade-specific LoS events. If a conserved EP pair flanked a breakpoint unique to a clade, the pair was considered split by the rearrangement. For clades such as Chiroptera, Perissodactyla, Afrotheria, and the suborder Hystricomorpha, for which the enhancer orthologs were not included in the dataset by Laverré et al, the coordinates were lifted over using the UCSC liftOver tool (https://genome-store.ucsc.edu/). To calculate the statistical significance of observed EP pair disruptions, we performed bootstrap by randomizations breakpoint coordinates across the human genome 1000 times while keeping the chromosomal distribution of breakpoints same as original set. The bootstrap-based p-values were obtained using:

$$p = \frac{1}{B}\left(1 + \sum_{b=1}^{B} (1)_{k_b > k}\right)$$

where B is the total number of bootstrap samples, k is the observed number of disrupted EP pairs.

Hi-C analysis

We used HUGIn web browser (https://yunliweb.its.unc.edu/hugin/tutorial_page.php), to fetch virtual 4C interaction profiles at 40 kb resolution from human Hi-C data across relevant tissues. For mouse (mm10), .cool files were obtained from the 4D Nucleome Data Portal (https://data.4dnucleome.org/) and virtual 4C profiles were generated using Fit-Hi-C (https://github.com/ay-lab/fithic). We downloaded chromatin compartment (A/B) files for both human and mouse tissues from the 4D Nucleome. Change in compartment along the genomic regions spanning the break-points was calculated using Kronecker's delta function:

$$\delta_{ij} \equiv \begin{cases} 0 & \text{for } i \neq j \\ 1 & \text{for } i = j. \end{cases}$$

If consecutive genomic bins i and j had same compartment (A-A or B-B), the function takes the value 1, and zero when i and j bins had different compartment values (A-B or B-A). We calculated the average and 95% confidence intervals of Kronecker's delta across all breakpoints for each tissue and clade (supplementary). For compact representation a global average of Kronecker's delta was plotted at 250 kb resolution around +/- 1 Mb to the break-point.

The source of all datasets used are listed in Dataset S2.

Data availability

All data generated or analysed during this study are included in its supplementary dataset files.

Competing interest statement

The authors declare that they have no competing interests

Acknowledgements

Authors duly acknowledge the financial support from Department of Biotechnology, India (BT/PR40149/BTIS/137/36/2022, BT/PR40198/BTIS/137/56/2023). JB performed all the data analysis and prepared the figures. ML helped in coding. KSS conceived, improvised, and guided the work, and wrote the manuscript.

References:

Akhtar W, de Jong J, Pindyurin A V, Pagie L, Meuleman W, de Ridder J, Berns A, Wessels LFA, van Lohuizen M, van Steensel B. 2013. Chromatin position effects assayed by thousands of reporters integrated in parallel. *Cell* **154**: 914–27.

Bagadia M, Chandradoss KR, Jain Y, Singh H, Lal M, Sandhu KS. 2019. Evolutionary Loss of Genomic Proximity to Conserved Noncoding Elements Impacted the Gene Expression Dynamics During Mammalian Brain Development. *Genetics* **211**: 1239–1254. http://www.ncbi.nlm.nih.gov/pubmed/30796012.

Bedell MA, Brannan CI, Evans EP, Copeland NG, Jenkins NA, Donovan PJ. 1995. DNA rearrangements located over 100 kb 5' of the Steel (Sl)-coding region in Steel-panda and Steel-contrasted mice deregulate Sl expression and cause female sterility by disrupting ovarian follicle development. *Genes Dev* **9**: 455–70.

Benjamin A, Costa AN Da, Delaunois A, Rosseels ML, Valentin JP. 2015. Renal safety pharmacology in drug discovery and development. *Handb Exp Pharmacol* **229**.

Bittner NKJ, Mack KL, Nachman MW. 2021. Gene expression plasticity and desert adaptation in house mice*. *Evolution (N Y)* **75**.

Bozek K, Wei Y, Yan Z, Liu X, Xiong J, Sugimoto M, Tomita M, Pääbo S, Sherwood CC, Hof PR, et al. 2015. Organization and Evolution of Brain Lipidome Revealed by Large-Scale Analysis of Human, Chimpanzee, Macaque, and Mouse Tissues. *Neuron* **85**.

Chen X, Zhang J. 2016. The Genomic Landscape of Position Effects on Protein Expression Level and Noise in Yeast. *Cell Syst* **2**: 347–54.

Chiang C, Scott AJ, Davis JR, Tsang EK, Li X, Kim Y, Hadzic T, Damani FN, Ganel L, GTEx Consortium, et al. 2017. The impact of structural variation on human gene expression. *Nat Genet* **49**: 692–699.

De S, Teichmann SA, Babu MM. 2009. The impact of genomic neighborhood on the

evolution of human and chimpanzee transcriptome. *Genome Res* **19**: 785–94.
Derous D, Sahu J, Douglas A, Lusseau D, Wenzel M. 2021. Comparative genomics of cetartiodactyla: Energy metabolism underpins the transition to an aquatic lifestyle. *Conserv Physiol* **9**.
Dickinson H, Moritz K, Wintour EM, Walker DW, Kett MM. 2007. A comparative study of renal function in the desert-adapted spiny mouse and the laboratory-adapted C57BL/6 mouse: Response to dietary salt load. *Am J Physiol - Ren Physiol* **293**.
Diessler M, Ventureira M, Hernandez R, Sobarzo C, Casas L, Barbeito C, Cebral E. 2017. Differential expression and activity of matrix metalloproteinases 2 and 9 in canine early placenta. *Reprod Domest Anim* **52**.
Doherty A, de Magalhães JP. 2016. Has gene duplication impacted the evolution of Eutherian longevity? *Aging Cell* **15**.
Dunn-Fletcher CE, Muglia LM, Pavlicev M, Wolf G, Sun MA, Hu YC, Huffman E, Tumukuntala S, Thiele K, Mukherjee A, et al. 2018. Anthropoid primate–specific retroviral element THE1B controls expression of CRH in placenta and alters gestation length. *PLoS Biol* **16**.
Elgin SC, Reuter G. 2013. Position-effect variegation, heterochromatin formation, and gene silencing in Drosophila. *Cold Spring Harb Perspect Biol* **5**: a017780. http://www.ncbi.nlm.nih.gov/pubmed/23906716.
Fantes J, Redeker B, Breen M, Boyle S, Brown J, Fletcher J, Jones S, Bickmore W, Fukushima Y, Mannens M, et al. 1995. Aniridia-associated cytogenetic rearrangements suggest that a position effect may cause the mutant phenotype. *Hum Mol Genet* **4**: 415–422.
Flomen RH, Vatcheva R, Gorman PA, Baptista PR, Groet J, Barišić I, Ligutic I, Nižetić D. 1998. Construction and Analysis of a Sequence-Ready Map in 4q25: Rieger Syndrome Can Be Caused by Haploinsufficiency ofRIEG, but Also by Chromosome Breaks ≈90 kb Upstream of This Gene. *Genomics* **47**: 409–413.
Gbadegesin RA, Hall G, Adeyemo A, Hanke N, Tossidou I, Burchette J, Wu G, Homstad A, Sparks MA, Gomez J, et al. 2014. Mutations in the gene that encodes the F-Actin binding protein anillin cause FSGS. *J Am Soc Nephrol* **25**.
Guntawang T, Sittisak T, Kochagul V, Srivorakul S, Photichai K, Boonsri K, Janyamethakul T, Boonprasert K, Langkaphin W, Thitaram C, et al. 2021. Pathogenesis of hemorrhagic disease caused by elephant endotheliotropic herpesvirus (EEHV) in Asian elephants (Elephas maximus). *Sci Rep* **11**.
Hudson NJ, Baker ML, Hart NS, Wynne JW, Gu Q, Huang Z, Zhang G, Ingham AB, Wang L, Reverter A. 2014. Sensory rewiring in an echolocator: Genome-wide modification of retinogenic and auditory genes in the bat Myotis davidii. *G3 Genes, Genomes, Genet* **4**.
Jebb D, Huang Z, Pippel M, Hughes GM, Lavrichenko K, Devanna P, Winkler S, Jermiin LS, Skirmuntt EC, Katzourakis A, et al. 2020. Six reference-quality genomes reveal evolution of bat adaptations. *Nature* **583**.
Jezova D, Ochedalski T, Glickman M, Kiss A, Aguilera G. 1999. Central corticotropin-releasing hormone receptors modulate hypothalamic- pituitary-adrenocortical and sympathoadrenal activity during stress. *Neuroscience* **94**.
Jiang Y, Xie M, Chen W, Talbot R, Maddox JF, Faraut T, Wu C, Muzny DM, Li Y, Zhang W, et al. 2014. The sheep genome illuminates biology of the rumen and lipid metabolism. *Science (80-)* **344**.
Kawai YK, Sano K, Ikenaka Y, Nakayama SMM, Kondo M, Kubota A, Ishizuka M. 2021. Evolutionary history of mammalian UDP-glucuronosyltransferase (UGT)1 and UGT2 families: the emergence of UGT2B subfamily in eutherians after the diversification of

flowering plants. *bioRxiv*.
Kim J, Farré M, Auvil L, Capitanu B, Larkin DM, Ma J, Lewin HA. 2017. Reconstruction and evolutionary history of eutherian chromosomes. *Proc Natl Acad Sci U S A* **114**: E5379–E5388.
Kleinjan DJ, Van Heyningen V. 1998. Position effect in human genetic disease. *Hum Mol Genet* **7**.
Krebs I. 1997. Translocation breakpoint maps 5 kb 3' from TWIST in a patient affected with Saethre-Chotzen syndrome. *Hum Mol Genet* **6**: 1079–1086.
Laverré A, Tannier E, Necsulea A. 2022. Long-range promoter–enhancer contacts are conserved during evolution and contribute to gene expression robustness. *Genome Res* **32**.
Lewis JH. 1974. Comparative hematology: Studies on elephants, Elephas maximus. *Comp Biochem Physiol -- Part A Physiol* **49**.
Liu W, Zhu P, Li M, Li Z, Yu Y, Liu G, Du J, Wang X, Yang J, Tian R, et al. 2023. Large-scale across species transcriptomic analysis identifies genetic selection signatures associated with longevity in mammals. *EMBO J* **42**.
Luo H, Arndt W, Zhang Y, Shi G, Alekseyev MA, Tang J, Hughes AL, Friedman R. 2012. Phylogenetic analysis of genome rearrangements among five mammalian orders. *Mol Phylogenet Evol* **65**: 871–82.
Milot E, Fraser P, Grosveld F. 1996. Position effects and genetic disease. *Trends Genet* **12**.
Muntané G, Horvath JE, Hof PR, Ely JJ, Hopkins WD, Raghanti MA, Lewandowski AH, Wray GA, Sherwood CC. 2015. Analysis of synaptic gene expression in the neocortex of primates reveals evolutionary changes in glutamatergic neurotransmission. *Cereb Cortex* **25**.
Nishibori Y, Katayama K, Parikka M, Oddsson Á, Nukui M, Hultenby K, Wernerson A, He B, Ebarasi L, Raschperger E, et al. 2011. Glcci1 deficiency leads to proteinuria. *J Am Soc Nephrol* **22**.
Pays E. 2021. The function of apolipoproteins L (APOLs): relevance for kidney disease, neurotransmission disorders, cancer and viral infection. *FEBS J* **288**.
Poole DC, Erickson HH. 2011. Highly athletic terrestrial mammals: Horses and dogs. *Compr Physiol* **1**.
Pusey A, Williams J, Goodall J. 1997. The influence of dominance rank on the reproductive success of female chimpanzees. *Science (80-)* **277**.
Real FM, Haas SA, Franchini P, Xiong P, Simakov O, Kuhl H, Schöpflin R, Heller D, Moeinzadeh MH, Heinrich V, et al. 2020. The mole genome reveals regulatory rearrangements associated with adaptive intersexuality. *Science (80-)* **370**.
Roth LS V, McGreevy P. 2025. Horse vision through two lenses: Tinbergen's Four Questions and the Five Domains. *Front Vet Sci* **12**: 1647911.
Sapolsky RM. 2021. Glucocorticoids, the evolution of the stress-response, and the primate predicament. *Neurobiol Stress* **14**.
Savage VM, Allen AP, Brown JH, Gillooly JF, Herman AB, Woodruff WH, West GB. 2007. Scaling of number, size, and metabolic rate of cells with body size in mammals. *Proc Natl Acad Sci U S A* **104**.
Singh A, Bagadia M, Sandhu KS. 2016. Spatially coordinated replication and minimization of expression noise constrain three-dimensional organization of yeast genome. *DNA Res* **23**: 155–169. http://www.ncbi.nlm.nih.gov/pubmed/26932984.
Smith R, Nicholson RC. 2007. Corticotrophin releasing hormone and the timing of birth.

Front Biosci **12**.
Spanaki C, Sidiropoulou K, Petraki Z, Diskos K, Konstantoudaki X, Volitaki E, Mylonaki K, Savvaki M, Plaitakis A. 2024. Glutamate-specific gene linked to human brain evolution enhances synaptic plasticity and cognitive processes. *iScience* **27**.
Sulak M, Fong L, Mika K, Chigurupati S, Yon L, Mongan NP, Emes RD, Lynch VJ. 2016. TP53 copy number expansion is associated with the evolution of increased body size and an enhanced DNA damage response in elephants. *Elife* **5**. http://www.ncbi.nlm.nih.gov/pubmed/27642012.
Tomas NM, Beck LH, Meyer-Schwesinger C, Seitz-Polski B, Ma H, Zahner G, Dolla G, Hoxha E, Helmchen U, Dabert-Gay A-S, et al. 2014. Thrombospondin Type-1 Domain-Containing 7A in Idiopathic Membranous Nephropathy. *N Engl J Med* **371**.
Wallrath LL, Elgin SC. 1995. Position effect variegation in Drosophila is associated with an altered chromatin structure. *Genes Dev* **9**: 1263–1277. http://www.ncbi.nlm.nih.gov/pubmed/7758950.
Wang H, Zhao H, Sun K, Huang X, Jin L, Feng J. 2019. Evolutionary Basis of High-Frequency Hearing in the Cochleae of Echolocators Revealed by Comparative Genomics. *Genome Biol Evol* **12**.
Wirth J, Wagner T, Meyer J, Pfeiffer RA, Tietze H-U, Schempp W, Scherer G. 1996. Translocation breakpoints in three patients with campomelic dysplasia and autosomal sex reversal map more than 130 kb from SOX9. *Hum Genet* **97**: 186–193.
Wooding FBP, Burton GJ. 2008. *Comparative placentation: Structures, functions and evolution*.
Xu Z, Lee D-S, Chandran S, Le VT, Bump R, Yasis J, Dallarda S, Marcotte S, Clock B, Haghani N, et al. 2022. Structural variants drive context-dependent oncogene activation in cancer. *Nature* **612**: 564–572.